

1 Analysis of Multisensory-Motor 2 Integration in Olfactory Navigation 3 of Silkmoth, *Bombyx mori*, using 4 Virtual Reality System

5 Mayu Yamada^{1†}, Hirono Ohashi^{1‡}, Koh Hosoda^{1‡}, Daisuke Kurabayashi^{2‡},
6 Shunsuke Shigaki^{1*}

*For correspondence:

shigaki@arl.sys.es.osaka-u.ac.jp (SS)₇

[†]These authors contributed
equally to this work

[‡]These authors also contributed
equally to this work

₈ ¹Department of System Innovation, Osaka University; ²Department of Systems and
Control Engineering, Tokyo Institute of Technology

₁₀ **Abstract** Most animals survive and thrive due to navigation behavior to reach their
₁₁ destinations. In order to navigate, it is important for animals to integrate information obtained
₁₂ from multisensory inputs and use that information to modulate their behavior. In this study, by
₁₃ using a virtual reality (VR) system for an insect, we investigated how an adult silkworm integrates
₁₄ visual and wind direction information during female search behavior (olfactory behavior).
₁₅ According to the behavioral experiments using the VR system, the silkworm had the highest
₁₆ navigation success rate when odor, vision, and wind information were correctly provided.
₁₇ However, we found that the success rate of the search significantly reduced if wind direction
₁₈ information was provided that was incorrect from the direction actually detected. This indicates
₁₉ that it is important to acquire not only odor information, but also wind direction information
₂₀ correctly. In other words, Behavior was modulated by the degree of co-incidence between the
₂₁ direction of arrival of the odor and the direction of arrival of the wind, and posture control
₂₂ (angular velocity control) was modulated by visual information. We mathematically modeled the
₂₃ modulation of behavior using multisensory information and evaluated it by simulation. As a
₂₄ result, the mathematical model not only succeeded in reproducing the actual female search
₂₅ behavior of the silkworm, but can also improve search success relative to the conventional odor
₂₆ source search algorithm.

₂₈ Introduction

₂₉ In many organisms, including humans, appropriate behavior is determined based on the integra-
₃₀ tion of different kinds of information from the environment. Examples of information obtained
₃₁ from the environment include light, sound, odor, and wind. Odor, unlike sound and light, does
₃₂ not have high temporal or spatial resolution, but is highly persistent and diffusive, and is there-
₃₃ fore widely used as a communication tool by organisms (*Renou, 2014*). Insects, in particular, com-
₃₄ municate extensively using odor (e.g., aggregation pheromone, trail pheromone, sex pheromone;
₃₅ (*Wyatt, 2014*)), despite their small-scale neural systems. Odor information is also largely used to
₃₆ locate feeding sites and flowers (*Renou, 2014*).

₃₇ Understanding odor-based search behavior is of great value not only in biology, but also in en-
₃₈ gineering research. This is because odor-based search can be applied to gas leak source search
₃₉ robots or lifesaving robots in a disaster area instead of dogs. There have been many attempts

40 to model the search behavior of living organisms using odor and to implement (**Chen and Huang,**
41 **2019**) it in robots, but artificial systems have not yet demonstrated the same capabilities as liv-
42 ing organisms. One of the reasons for this lack of performance is that models do not incorporate
43 when and under what conditions, and which sensory information is fed back to inform subsequent
44 behavior. To solve this problem, it is necessary to measure behavioral changes in insects when
45 multiple types of sensory information are presented to them. Previously, Pansopha *et al.* (**Pan-**
46 **sopha et al., 2014**) found that the mating behavior of a silkmoth, which is elicited by odor stimulus,
47 was modulated by visual stimulus. Further, in a study on crickets, Haberkern *et al.* (**Haberkern**
48 **and Hedwig, 2016**) reported that long-term tactile stimulation suppressed phototaxis, suggesting
49 that behavioral switching between proximal environmental information and phototaxis may occur.
50 These results revealed that behavioral modulation and switching mechanisms occur in all insects
51 through the acquisition of multiple types of environmental information. However, because these
52 experimental results were obtained when controlled stimuli were provided, the mechanisms of be-
53 havioral modulation and switching when complex environmental changes were presented are still
54 unknown. In recent years, the use of virtual reality (VR) systems in insect behavioral experimental
55 setups has attracted attention as a way to present complex environmental changes. For example,
56 Kaushik *et al.* (**Kaushik et al., 2020**) found that dipterans use airflow and odor information for vi-
57 sual navigation using an insect VR system. Because VR systems allow for the presentation of more
58 natural environmental changes, they also allow for quantitative analysis of the effect of behavior
59 modulation and switching mechanisms on functions such as search and navigation. Furthermore,
60 they allow researchers to create and test insects in situations that do not occur in nature, and may
61 therefore play an important role in the construction of robust behavioral decision algorithms for
62 unknown environments.

63 In order to elucidate the adaptive odor source search behavior of insects, we constructed a
64 VR system that can present multiple types of environmental information simultaneously and con-
65 tinuously, and employed it to clarify how sensory information other than odor is used. Our VR
66 system was connected to a virtual field built on a computer, and presented odor, wind, and visual
67 stimuli according to environmental changes in the virtual search field. We employed an adult male
68 silkmoth *Bombyx mori* as our measurement target. Female search behavior of the silkmoth has
69 a stereotyped pattern (**Ryohei et al., 1992**), but the duration and speed of the behavior are regu-
70 lated by the frequency of odor detection and the input of other sensory information (**Pansopha**
71 **et al., 2014; Shigaki et al., 2019a,b**). However, previous studies have observed silkmoth behavior
72 in response to a specified, unchanging amount of stimulus, and the nature of behavioral changes
73 during an actual odor source search warrants further investigation.

74 In this study, we used a VR system to clarify which sensory organs the silkworm moth uses to
75 search for females, and how they are used. In addition, we constructed a model from our biological
76 data and tested the validity of the model using a constructive approach.

77 Results

78 In this study, we analyzed changes in female search behavior of an adult male silkmoth in response
79 to multiple sensory inputs. To measure behavior, we constructed a novel virtual reality device that
80 presents odor, visual, and wind stimuli (Fig. 1A) to provide the silkmoth with the illusion that it
81 was searching for a female (see Supplemental video 1). The providing for each sensory input is
82 defined as shown in Fig. 1B. The odor discharge port is integrated with a tethered rod for fixing
83 the body, and the sex pheromone is discharged independently from the upper part of the left and
84 right antennae. The direction of wind stimulation is determined by the heading angle with respect
85 to the windward direction from the four directions: front, back, left and right. Moreover, the visual
86 stimulus provides an optical flow in the direction opposite to the turn direction. The VR device
87 was connected to a virtual field built on a computer, and the odor puffs in the virtual field were
88 produced by image processing of the actual odor diffusion using an airflow visualization system
89 (**Yanagawa et al., 2018**). In addition, the virtual field was set with wind flowing uniformly from left

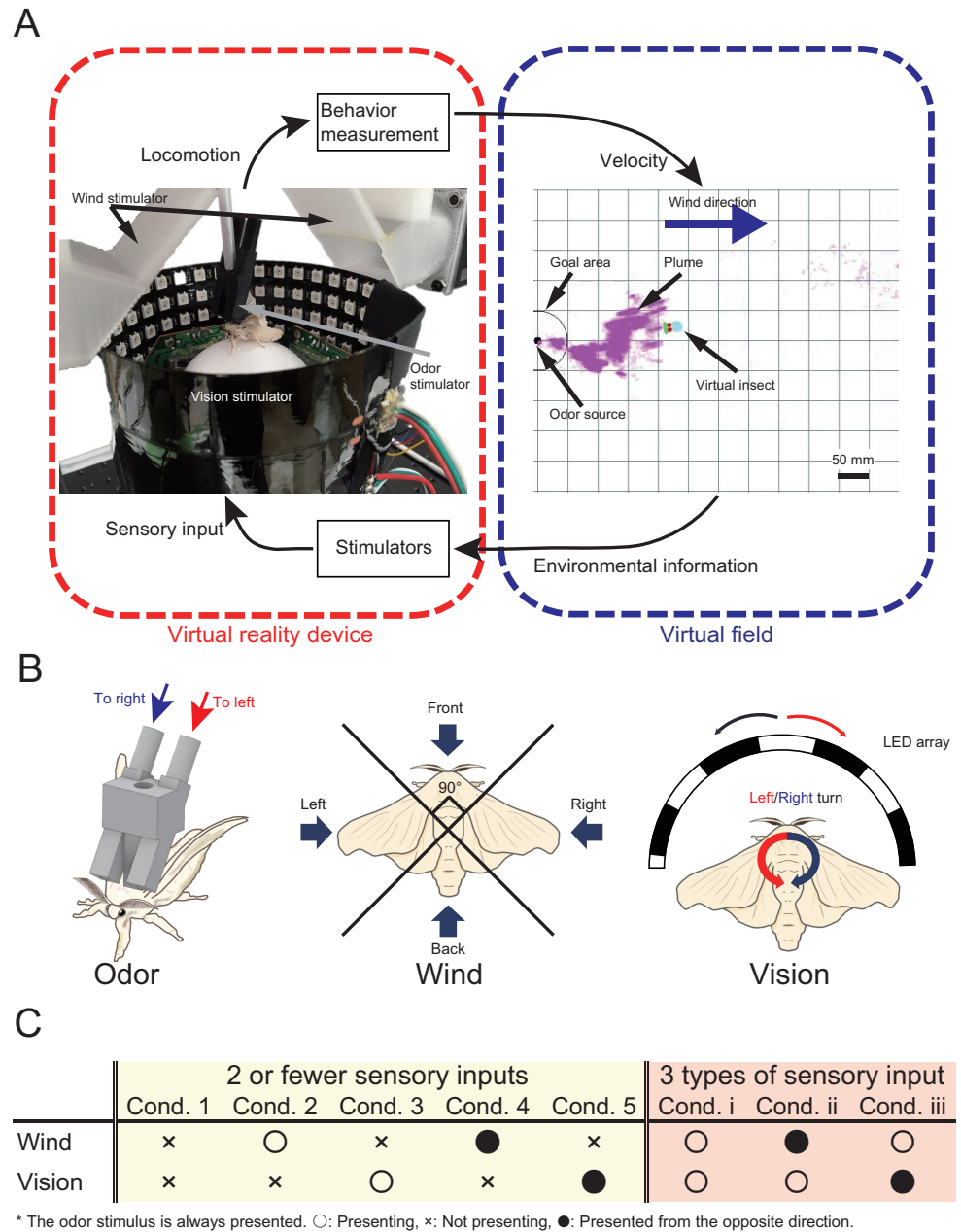


Figure 1. The virtual reality (VR) system for olfactory navigation of the insect and a list of experimental conditions. A: The VR system is equipped with a stimulator of odor, vision, and wind, and is connected to a virtual odor field. The insect on the VR device performs olfactory navigation in virtual space. B: Definition of presentation way of each sensory stimulus. C: The odor is presented under all conditions. "○", "x", and "●" indicate presented, not presented, and presented from the opposite direction to the actual direction, respectively.

Figure 1-Figure supplement 1. System configuration diagram and evaluation of VR system.

Figure 1-video 1. A video of a silkworm behavior experiment using a VR system.

90 to right. The search performance of the silkmoth using the constructed VR system was the same as
91 that in free-walking experiments (see Supplemental Materials). We carried out experiments using
92 the VR by changing the number of sensory inputs as follows (Fig. 1C);

- 93 • Presents two or less types of sensory input (Group1: odor only / odor + wind / odor + vision),
- 94 • Presents three types of sensory input (Group2: odor + wind + vision) .

95 "o" indicates that we presented the environmental information to the silkmoth, and "x" indi-
96 cates that we did not present the environmental information to the silkmoth (Fig. 1C). "•" indicates
97 that the stimulus was presented from the opposite direction. For example, "Inverse wind" means
98 that the virtual insect in the computer received wind from the front, while the real silkmoth received
99 wind from the back. Three repetitions of the experiment were conducted using 10 silkworm moths
100 for each environmental condition ($n=30$). We set a time limit of 300 seconds because theoretically,
101 the silkmoth could reach the odor source in an infinite time. The search was considered a failure
102 if the moth did not enter a radius of 10 mm from the odor source within the time limit.

103 **Wind and visual effects on the olfactory navigation**

104 We compared the search performance in response to different types of stimuli by presenting wind
105 and visual stimuli in addition to olfactory stimulus in all conditions. We first measured the behavior
106 when wind or visual stimuli is providing in addition to odor stimulus (Group 1). We created a migra-
107 tion probability map in order to visualize the effects of differences in environmental conditions on
108 the behavioral trajectory (Fig. 2A—E). To quantitatively evaluate the similarity between the migra-
109 tion probability maps, we calculated the earth mover's distance (EMD) (*Rubner et al., 1997*). EMD
110 is an index that calculates whether the distributions of two histograms are similar. The smaller the
111 EMD value, the more similar the two histograms, and the larger the value, the less similar. Fig. 3F
112 shows the result of calculating EMD based on cond. 1, in which only the odor stimulus was pre-
113 sented. The silkmoths' trajectory in cond. 3 and 5 (odor + vision) was very similar to the trajectory in
114 cond. 1 (only odor), suggesting that vision did not significantly affect search behavior. In addition,
115 the EMD value when wind stimulus was presented in addition to odor was > 10 , suggesting that
116 the addition of wind stimulus did significantly affect search behavior. We illustrated the navigation
117 success rate and search time (yellow background in Fig. 3A and B). Additionally, we calculated the
118 search success rate per unit time (SPT) as a measure of the relationship between the search suc-
119 cess rate and search time (yellow background in Fig. 3C). Higher SPT values represent better search
120 performance. It was found that the success rate was most improved when the wind was presented
121 correctly (cond. 2) compared to when only the odor stimulus was provided (cond. 1). The success
122 rate was lower under the condition where the wind was presented from the direction opposite to
123 the direction detected in the virtual environment (cond. 4), compared with the condition where
124 only odor stimulus was presented (cond. 1). Moreover, SPT in cond. 3 and 5, in which the direction
125 of the visual stimulus was changed without presenting the wind stimulus, were almost the same
126 (0.411 vs. 0.409), suggesting that visual stimulus had little effect on the search performance. From
127 this, it was found that the success rate of navigation tends to improve by correctly presenting wind
128 stimulus in addition to the odor.

129 We found that when three types of sensory stimuli were presented (Group2), the success rate
130 changed significantly compared to when two types of sensory stimuli were presented (red back-
131 ground in Fig. 3). Focusing on cond. i, the SPT values were also significantly different, suggesting
132 that the olfactory navigation can be performed more accurately and efficiently by presenting all
133 sensory stimuli. Additionally, under the condition that the wind stimulus is presented from the
134 direction opposite to the direction received in the virtual environment, the search success rate is
135 significantly reduced, and it is clear that the wind direction information is an important factor. To-
136 gether, we hypothesized that the silkmoth has achieved efficient female search using all sensory
137 inputs: odor, wind, and vision.

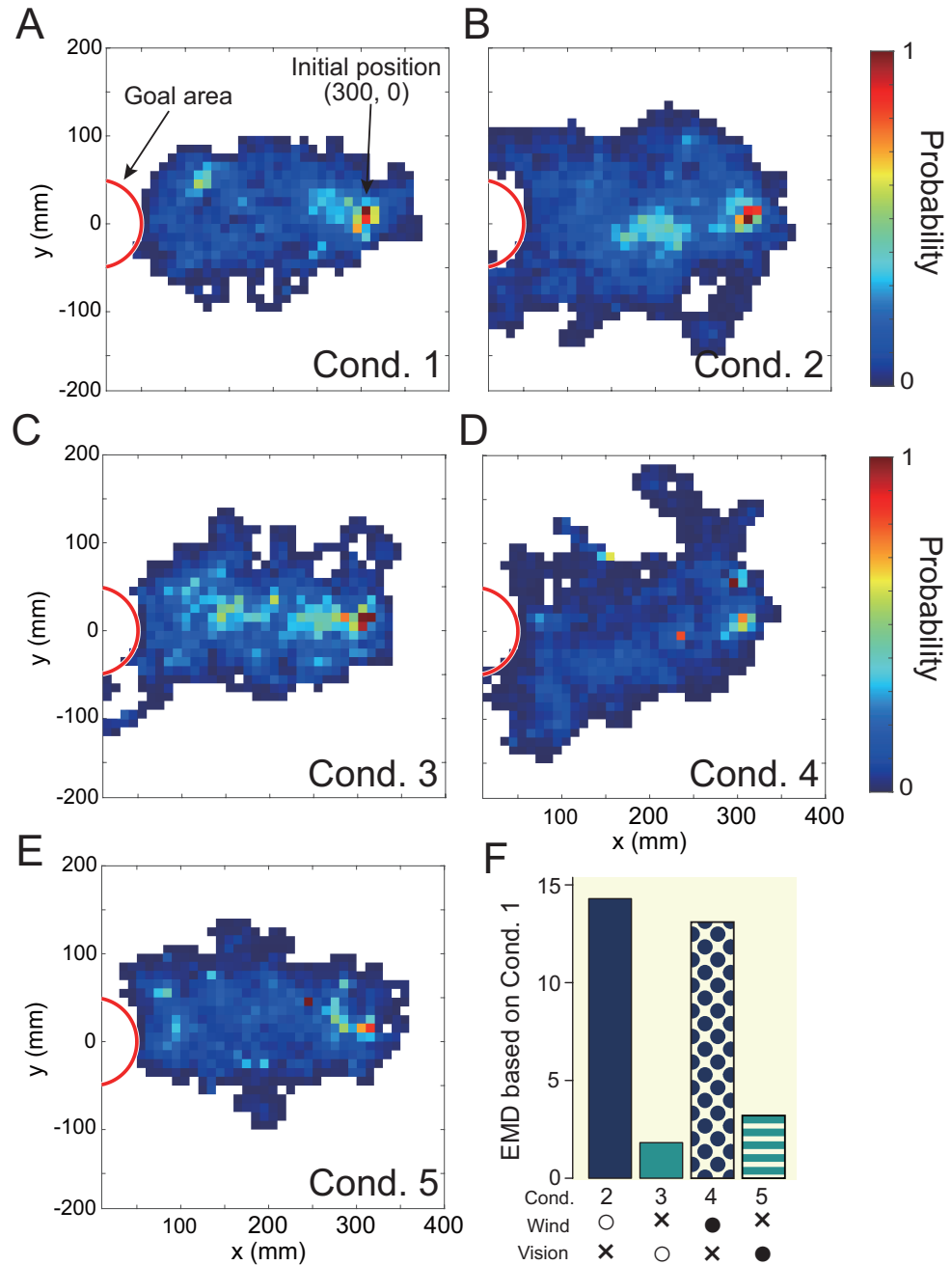


Figure 2. The result of visually expressing the trajectory under each experimental condition with a migration probability map (A—E). The white area in the figure indicates that the moth did not move in that space. A quantitative evaluation using earth mover's distance, EMD is illustrated in F. F was the result of calculating the similarity (EMD) based on the trajectory of cond. 1 (odor presentation only). The lower the value, the higher the similarity, and the higher the value, the lower the similarity of the trajectories.

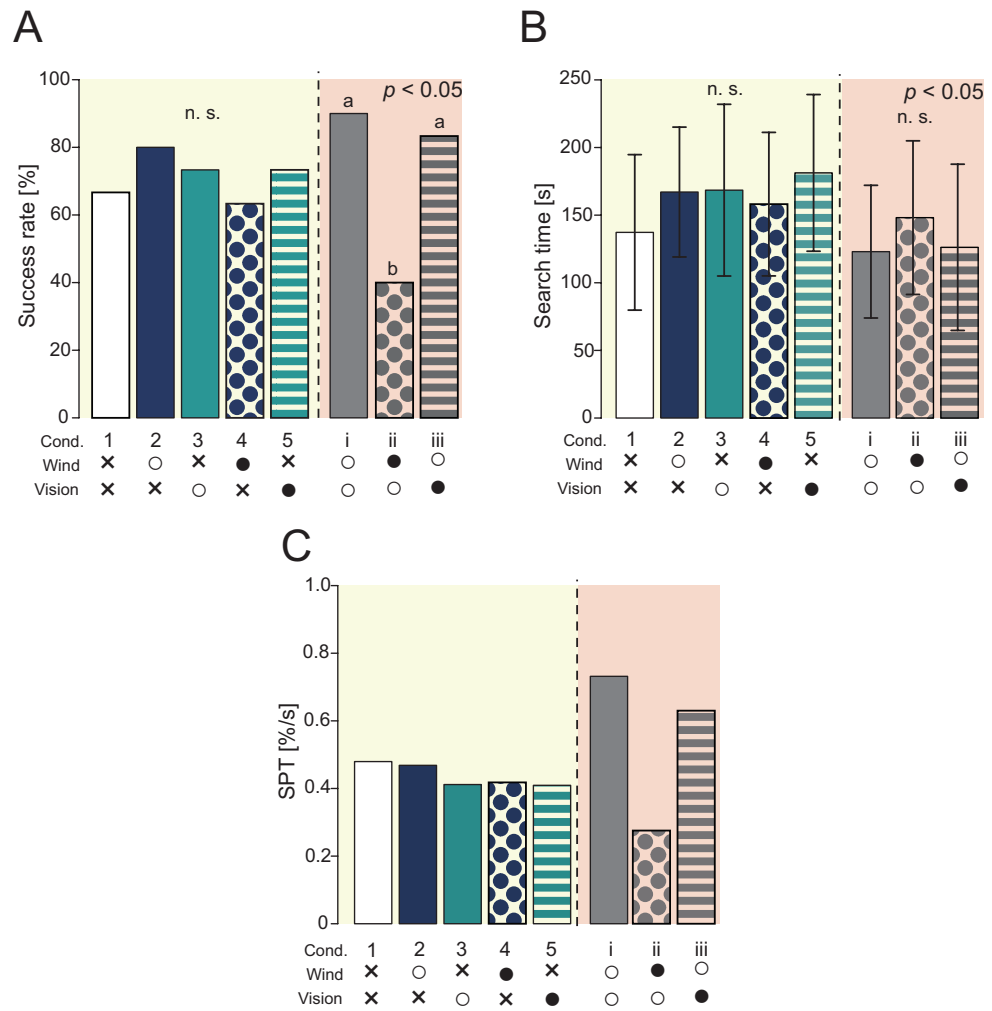


Figure 3. Results of navigation experiments using virtual reality (VR). The yellow background is the result of providing 2 or fewer sensory stimuli, and the red background is the result of providing 3 sensory stimuli. A: The success rate of the navigation (Fisher's exact test, $p < 0.05$). B: The search time at the time of success (Steel-Dwass test, $p < 0.05$). C: Search performance. The success rate per unit time was calculated based on the results of A and B.

138 **Extraction of behavioral modulation mechanisms in the odor source search**

139 In the previous section, it was found that wind direction information, in addition to odor informa-
140 tion, contributed to improving the success rate in searching for the odor source. Here, we analyze
141 in detail how behavior is modulated by visual and wind information using three experimental con-
142 ditions: a forward condition (cond. i), an inverse condition for wind direction information (cond. ii),
143 and an inverse condition for visual stimuli (cond. iii).

144 We first analyzed the effect of wind direction information on odor source search behavior. The
145 results of calculating EMD in the previous section suggested that the search behavior was signif-
146 icantly affected when wind direction information was presented, in addition to odor information.
147 Because the key stimulus for female searching behavior in silkmoths is odor, and because previ-
148 ous studies (e.g. (*Kikas et al., 2001*)) have reported that odor detection frequency is related to the
149 distance from the odor source, and that odor detection frequency modulates behavior, we ana-
150 lyzed odor as a state variable. Here, odor detection frequency is defined as the frequency at which
151 the silkmoth receives odors per unit of time. Fig. 4A shows a boxplot of the relationship between
152 odor detection frequency and movement speed when wind direction information is presented in
153 the forward direction. Fig. 4B shows the results when the wind direction information in the virtual
154 and real environments is presented in opposite directions. The black dot in the white box repre-
155 sents the average value. In Fig. 4A and B, the horizontal axis represents odor detection frequency,
156 and the vertical axis represents the translational and angular velocities. The red box plot in the
157 figure shows the peak velocity. When the direction of the wind in the virtual environment and the
158 direction of the wind presented to the silkmoth in the real environment matched, odor detection
159 frequency peaked at 0.7 Hz. However, in the non-matching condition, the silkmoths always moved
160 at a constant speed, regardless of the odor detection frequency. The angular velocity peaked at 0.4
161 Hz in the matched condition but shifted to 0.2 Hz in the non-matched condition. The peak transla-
162 tional velocity was very close to the frequency of female sex pheromone emission (approximately
163 0.8 Hz (*Fujiwara et al., 2014*)). When odor detection frequency was low, the female was far from
164 the male, and therefore the male searched actively. However, as the distance from the female
165 decreased, the frequency approached 0.7 Hz, which suggests that the male may be trying to locate
166 the female more carefully by increasing the spatiotemporal resolution of the search. On the other
167 hand, when the wind and odor directions do not coincide, the silkmoth may try to stay within the
168 reach of the odor by constantly searching regardless of the odor detection frequency. This may
169 be because the peak of the angular velocity shifts toward a lower odor detection frequency, and if
170 the odor and wind direction do not match, the silkmoth rotates slowly to carefully search for the
171 odor.

172 Next, we investigated the effects of visual stimuli on odor source search behavior. Section 2.1
173 suggests that visual stimuli do not directly contribute to search performance. However, many fly-
174 ing insects with compound eyes use visual information for their own postural control (*Dyhr and*
175 *Higgins, 2010*)(*Dyhr et al., 2013*). The silkmoth, although a walking insect, may retain some vestiges
176 of flying insects (*Kanzaki, 1998*)(*Shigaki et al., 2016*). Therefore, we hypothesized that vision may
177 be used for postural control. To test this hypothesis, we compared the angular velocities of silk-
178 moths in cond. i (all stimuli in the forward direction) to those in cond. iii (visual stimuli presented in
179 the inverse direction). Fig. 4C shows a histogram of the left and right angular velocities under each
180 experimental condition. The red color in Fig. 4C indicates the angular velocity when rotating coun-
181 terclockwise, and the blue color shows the angular velocity when rotating clockwise. The position
182 of the vertical bar above the histogram represents the average angular velocity, and the length of
183 the horizontal bar represents the standard deviation. Although the average angular velocities of
184 the left and right rotations were the same in cond. i (visual stimuli presented correctly), the angu-
185 lar velocities of the left and right rotations differed when the visual stimuli were presented in the
186 opposite direction to reality (Wilcoxon rank sum statistical test, $p < 0.05$). These results indicate
187 that silkmoths, like flying insects, use visual stimuli for postural control.

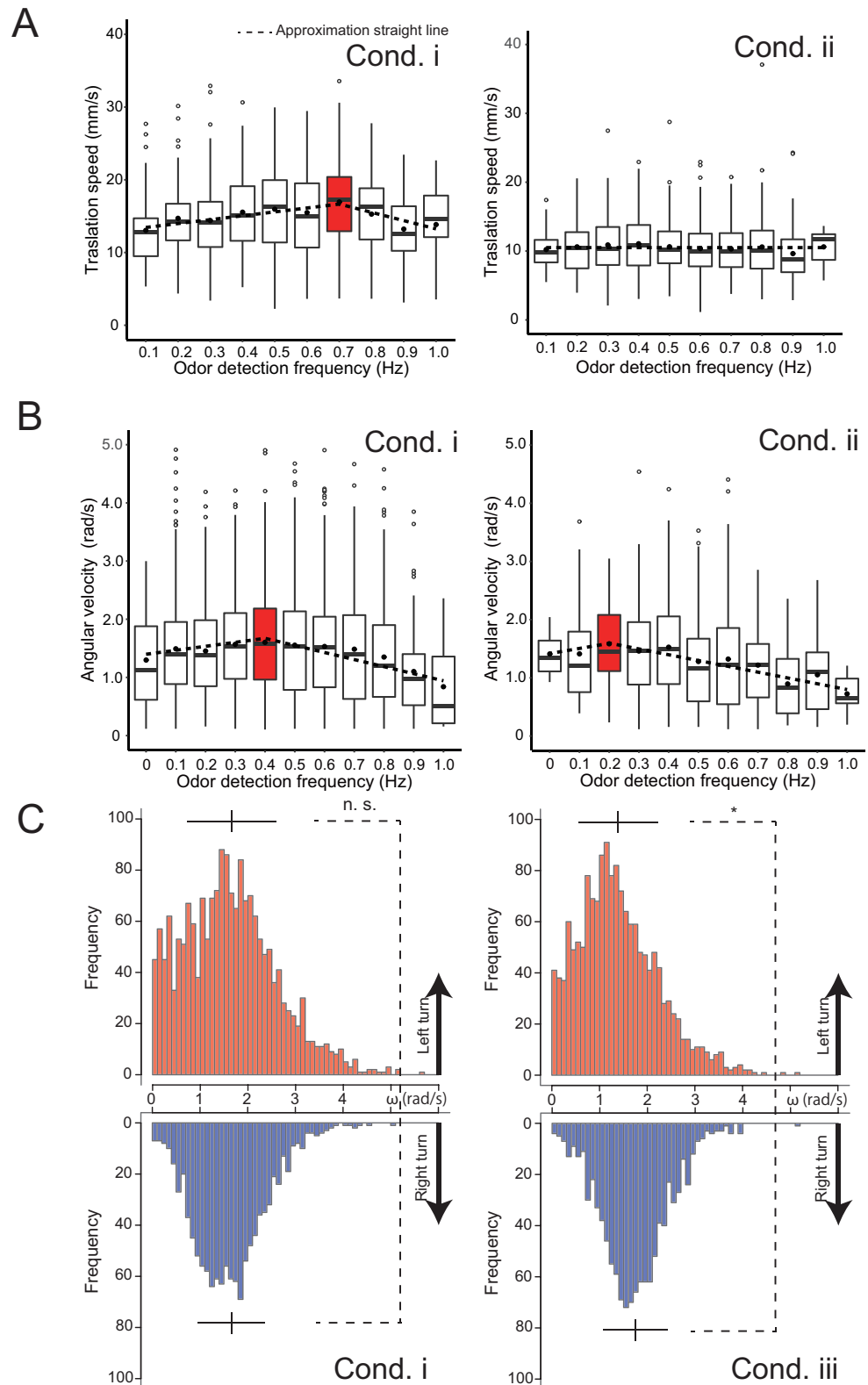


Figure 4. Analysis of the effects of wind and vision direction on behavior. A: Changes in the translational velocity and angular velocity when the wind direction was presented correctly (cond. i). Both translation and angular velocity peaked, and the behavior was modulated depending on the odor detection frequency. B: Changes in translational velocity and angular velocity when the wind was presented from the direction opposite to the actual direction (cond. ii). The translational velocity was constant regardless of the odor detection frequency, and the peak position of the angular velocity was 0.5 times that of cond. i. C: Comparison of angular velocities when the visual information was presented correctly (cond. i) and when it was presented in the opposite direction (cond. iii). Vision was used to equalize the speed of the left-right rotation.

188 We found that the silkmoth modulated its behavior based on whether or not the direction of
189 odor and wind detection coincided.

190 Modeling and validation of behavioral modulation mechanisms

191 Here, we investigated how behavioral modulation obtained from behavioral experiments using a
192 VR system contributes to the odor source search. A silkmoth moves by walking on a two-dimensional
193 plane with six legs, but it does not move in the lateral direction. Therefore, we assumed that it has
194 non-holonomic constraints and constructed our model to output straight-ahead and rotational
195 movements. Previous studies have proposed a silkmoth search model called the surge-zigzagging
196 algorithm (*Ryohei et al., 1992*)(*Shigaki et al., 2019b*), which makes action decisions using only olfac-
197 tory information. In this study, we updated the surge-zigzagging algorithm to incorporate wind di-
198 rection information. For convenience, we called this algorithm MiM2 (the multisensory input-based
199 motor modulation) algorithm. A block diagram of the constructed MiM2 algorithm is presented in
200 Fig. 5A. The model has a straight-ahead speed (v) controller (1) and an angular velocity (ω) con-
201 troller (2), and each controller changes output depending on the amount of sensory information
202 input. The detailed equations for each controller are shown below:

$$v(t) = \frac{K_v(f) \times \exp(-(t - t_d))}{1 + \exp(\gamma((t - t_d) - \beta))} \quad (1)$$

$$\omega(t) = \frac{\omega_0 \times R_d(0)}{1 + \exp(\gamma((t - t_d) - \beta))} + \frac{K_\omega(f) \times R_d(N)}{1 + \exp(-\gamma((t - t_d) - \beta))} \quad (2)$$

$$K_{v/\omega}(f) = a_{v/\omega} \times f + b_{v/\omega} \quad (3)$$

Table 1. List of parameters for $K(f)$.

(a) K_v			(b) K_ω				
		a_v	b_v		a_ω	b_ω	
Odor direction	$f \leq 0.7$	5.36	12.9	Odor direction	$f \leq 0.4$	0.638	1.40
= Wind direction	$f > 0.7$	-11.4	24.6	= Wind direction	$f > 0.4$	-1.22	2.16
Odor direction	$f \leq 0.7$	0.0	10.5	Odor direction	$f \leq 0.4$	0.870	1.42
≠ Wind direction	$f > 0.7$	0.0	10.5	≠ Wind direction	$f > 0.4$	-0.997	1.80

203 The free parameters were set to $\gamma = 1000$, $\beta = 0.50$, and $\omega_0 = 0.57$. Here, f denotes the odor
204 detection frequency. Moreover, $K(f)$ is a linear function that varies with the direction of odor
205 detection and wind detection. The parameters a and b of $K(f)$ are shown in Table 1. These were
206 obtained by approximating the results of the behavioral experiment to the least-squares method
207 (Dotted line in Fig. 4A, B). In addition, t_d , R_d , and N represent the odor detection timing, the odor
208 detection direction, and the number of turn motions, respectively. $R_d(0)$ represents a straight-
209 ahead motion state and takes a value of -1 when the left antenna detects and 1 when the right
210 antenna detects. If both antennae detect, a value of -1 or 1 is randomly selected. N increases
211 according to Equation (4) up to four, but does not take a value of four or more because the number
212 of zigzagging motions was approximately three in a previous study (*Ryohei et al., 1992*). When
213 it receives an odor stimulus according to Equation (1-3), it generates a straight motion for 0.5
214 seconds and then makes a turn motion.

$$N(t) = [0.0116(t - t_d)^3 - 0.199(t - t_d)^2 + 1.1971(t - t_d) + 0.4482] \quad (4)$$

215 By passing through the directional discriminator and frequency counter, the odor is converted
216 into information such as whether it was detected by the left or right antennae and how much odor
217 it was exposed to. The wind is converted into wind direction information. A comparator is used

218 to determine whether the direction of odor detection and the direction of the wind are the same,
219 and the results are input to the straight-ahead speed and angular velocity controllers, which also
220 receive odor detection frequency. Visual information controls the angular velocity of the left and
221 right rotational movements following which olfactory behavior takes place. From this information,
222 the movement speed output is calculated, and the behavior is generated. We compared the MiM2
223 algorithm to the previous surge-zigzagging algorithm and the casting algorithm, which uses wind
224 information for searching in a moth-inspired algorithm proposed in a previous study (*Li et al.,*
225 *2001*).

226 The simulation environment employed a virtual environment similar to that used in the behav-
227 ioral experiments in the VR system (see Supplemental video 2). For each algorithm, we performed
228 1000 odor source search experiments to evaluate search success rate and trajectory. The results
229 are shown in Fig. 5B, C and D. Fig. 5B and C show the search success rate and the search time,
230 respectively. MiM2 algorithm showed a significantly higher search success rate than the other al-
231 gorithms (Fisher's exact test, $p < 0.05$). The casting algorithm showed the shortest search time
232 (Steel-Dwass test, $p < 0.05$) because it is an algorithm that actively moves upwind using odor detec-
233 tion. However, if the heading angle when moving upwind was incorrect, the search success rate
234 of this algorithm was the lowest of the three, because there was a high possibility that the agent
235 would have moved in the wrong direction. Next, we focus on the trajectory shown in Fig. 5E—H.
236 The black line in Fig. 5E—H shows the range that the odor has a high probability of reaching. The
237 search trajectory shows that the MiM2 algorithm always placed the searching agent in the middle
238 of the odor distribution, whereas the conventional surge-zigzagging and surge-casting algorithms
239 tended to place the searching agents near the edges of the odor. We evaluated the differences in
240 trajectory between algorithms quantitatively by calculating their EDMs (Fig. 5D). The comparison
241 of these EDM values suggested that the MiM2 algorithm most closely resembled actual silkmoth
242 movements, and was the closest to the results of behavioral experiments under the free walking
243 condition. Thus, the MiM2 algorithm can simulate search behavior similar to that of real silkmoths
244 by modulating the movement speed based on wind information in addition to odor and equalizing
245 the left-right angular velocities based on visual information.

246 Discussion

247 Virtual reality for insect behavior measurements

248 All animals, including insects, need to navigate for survival and reproduction. It is especially im-
249 portant to navigate efficiently in harsh environments and in situations in which there are many
250 competitors. Previous studies have investigated the homing behavior of a desert ant (*Cataglyphis*)
251 (*Wehner, 2003*), the pheromone source localization behavior of a male silkmoth (*Bombyx mori*)
252 (*OBARA, 1979*), and the sound source localization behavior of female crickets (*Gryllus campestris L.*)
253 (*Schmitz et al., 1982*). These studies have contributed to our understanding of the sensory-motor
254 integration mechanism that converts sensory input into motor output, an important function of
255 the neural system. However, the insects in these studies may not have displayed navigation behav-
256 ior as they would have under natural conditions, because stimuli were controlled and presented
257 in a fixed amount and at regular intervals in the behavioral experiments. In addition, the nature of
258 behavior change in a large-scale space and over a long period is relatively unknown because the be-
259 havioral experiments were carried out in a relatively small space and over a relatively short time.
260 Because of this, multimodal virtual reality (VR) systems have attracted a great deal of attention
261 (*Kaushik et al., 2020*)(*Naik et al., 2020*). The advantage of using a multimodal VR system is that not
262 only can behavior be measured at a large spatiotemporal scale, but the transmission of stimuli can
263 be precisely controlled and the behavioral output can be precisely measured. Biological data de-
264 scribing the relationship between sensory input and motor output are useful not only for clarifying
265 biological functions, but also for the field of robotics, because these data play a very important role
266 in modeling insect systems. Because the multimodal VR system in the previous studies was devel-

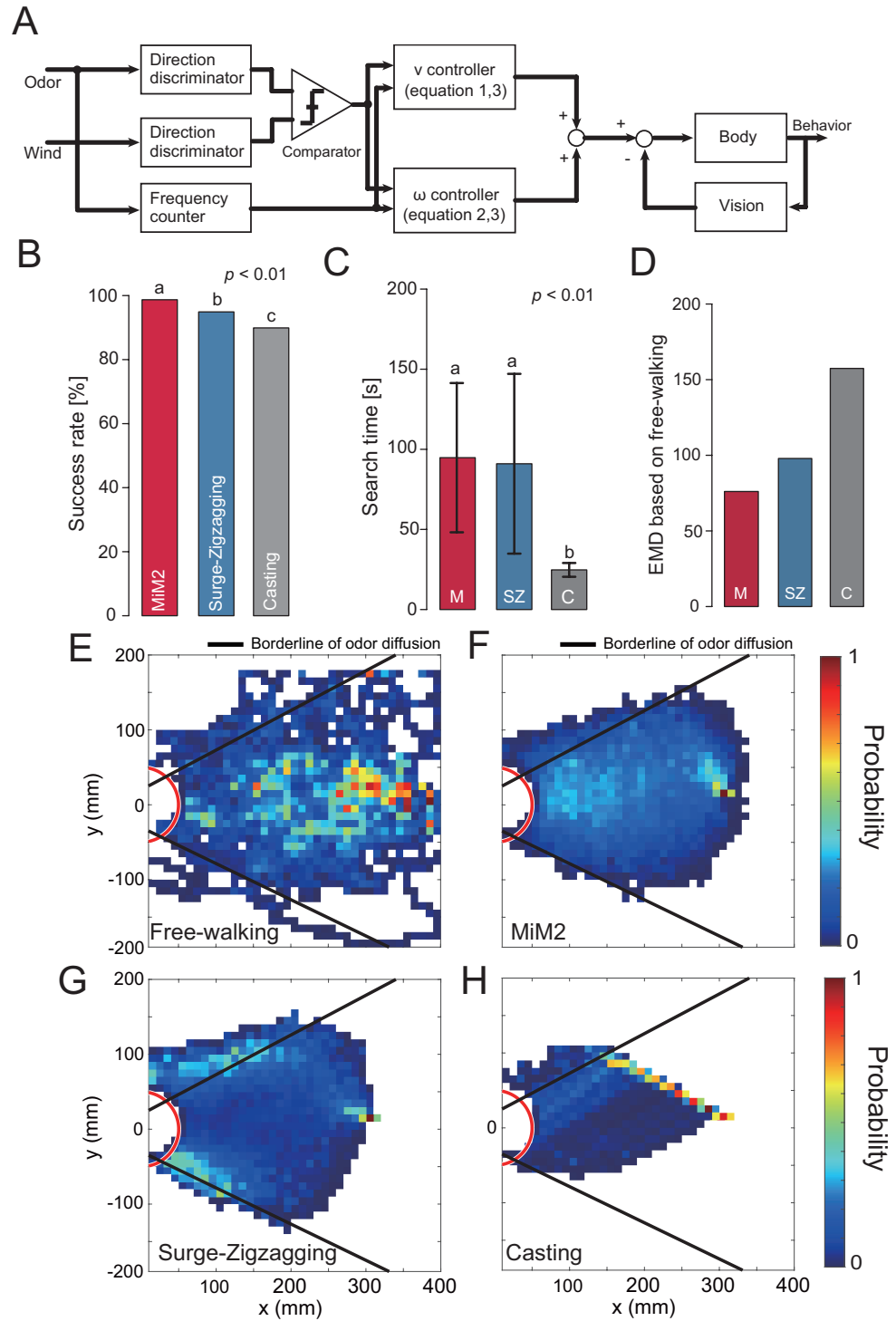


Figure 5. Block diagram of the proposed model and the simulation results. A: Cont2rol model that modulates speed according to the degree of coincidence between odor detection direction and wind direction. B: The success rate of navigation. C: The search time at the time of success. D: The EMD of each search algorithm calculated based on the migration probability map from the free-walking experiment. E—H: The migration probability map at the time of success.

Figure 5-Figure supplement 1. Flowchart of other algorithms.

Figure 5-video 1. Experimental video of the simulation.

267 oped for visual-dominated navigation, it was difficult to measure olfactory-dominated navigation,
268 which was the focus of our research. Therefore, we developed a novel multimodal VR system that
269 allowed us to measure changes in navigation behavior when the olfactory, visual, and wind direc-
270 tions of the silkmoth were modified. Conventionally, previous studies on the silkmoth have shown
271 that (1) a "mating dance" was elicited in response to sexual pheromones (*OBARA, 1979*), (2) the con-
272 dition in which visual stimuli was presented immediately after the reception of sex pheromones
273 influenced the subsequent rotational behavior (*Pansopha et al., 2014*), and (3) behavioral inhibition
274 occurred in response to frontal winds (*Shigaki et al., 2019a*). However, the integration of the above
275 phenomena during navigation has not been investigated. By presenting three types of sensory in-
276 formation simultaneously as well as continuously, we were able to clarify the roles of each type of
277 sensory information in navigation. Moreover, mathematical modeling and simulation showed that
278 multimodal sensory information improved silkmoth navigation.

279 **Behavioral modulation to odor frequency**

280 Organisms of all size scales rely on the ability to locate an odor source in space. The chemotaxis
281 of bacteria and a nematode have been determined by measuring and analyzing the relationship
282 between chemical stimulus input and behavioral output under a controlled environment (*Berg,*
283 *2008*)(*Lockery, 2011*). This study found that as the concentration of chemical stimuli increased, the
284 probability of rotating behavior decreased linearly. In other words, bacteria or nematode chemo-
285 taxis followed the odor gradient, which allowed them to locate the odor source. In the space where
286 bacteria and the nematode exist, chemotaxis is effective in part because the odor field of the en-
287 vironment does not change significantly due to wind. In the case of larger-scale animals, the odor
288 field of the environment is quite complex and it is difficult to reach the odor source by following
289 the gradient alone. Odor fields can be complex because odor molecules are transported by airflow
290 and mixed with other molecules at their destinations, forming complex structures (*Crimaldi and*
291 *Koseff, 2001*)(*Murlis et al., 1992*). In addition, the odor molecules themselves are discrete in space,
292 and do not carry information about the source of the odor. However, a study using a sensor ar-
293 ray to measure the arrival of odors carried by the wind revealed that the odors emitted from the
294 source arrive periodically (*Kikas et al., 2001*)(*Murlis et al., 2000*). Moreover, the periodicity is corre-
295 lated to some extent with the distance from the source; the closer the source, the shorter the cycle,
296 and the farther the source, the longer the cycle of arrival. Neither the concentration of the odor
297 nor the number of exposures played an important role in the search process in *drosophila*, but
298 the "tempo" at which flies encountered the odor was an important factor in the decision-making
299 process (*Celani, 2020*)(*Demir et al., 2020*). If we assume that the "tempo" is the rate of odor de-
300 tection per unit time, it is related to the cycle in which the odor arrives. We hypothesized that the
301 silkmoth, like flying insects such as *drosophila*, modulates its behavior based on the "tempo" of the
302 odor, therefore we included odor frequency in our analyses.

303 When the direction of the wind and the odor coincided, movement speed peaked when the
304 odor frequency was 0.7—0.8, which is similar to the frequency at which a female silkmoth releases
305 sex pheromones (0.79 ± 0.05 Hz) (*Fujiwara et al., 2014*). Based on these findings, we can hypothe-
306 size that if the male silkmoth detects wind and odor from the same direction, it correctly moves in
307 the direction of the female and actively searches the field until it reaches a location where the sex
308 pheromone release frequency approximates that of the female. When the frequency exceeded 0.8
309 Hz, the male seemed to be in the vicinity of the female and therefore increased the spatiotemporal
310 resolution of the search in order to locate the female and prepare for the transition to mating be-
311 havior. This might correspond to the silkmoth switching to the odor source declaration algorithm
312 in olfactory navigation. The biological experimental data obtained in this study are consistent with
313 those of earlier research demonstrating that an algorithm that shortens the travel distance of the
314 surge toward the end of the search improves the search performance of a robot (*Shigaki et al.,*
315 *2017*).

316 In an earlier study investigating the direction of wind and odor in the environment, the direc-

317 tion of wind and odor were the same in the open field experiment (no obstacles) (*Murlis et al.*,
318 *2000*). However, the direction of wind and odor is not always the same in a complex environment
319 such as a forest with many trees (*Murlis et al.*, *2000*). Our data showed that in situations where
320 the wind and odor direction do not match, the silkmoth always moves at the same rate given any
321 odor detection frequency. This may be a chemical tracking strategy to avoid leaving the odor range
322 by moving at a speed lower than normal speed, and suggests that the silkmoth is estimating the
323 degree of environmental turbulence and modulating its behavior based on the odor and wind di-
324 rection information. This strategy may be applicable to an engineering search system that switches
325 the search strategy according to the environmental conditions.

326 **Comparison with conventional CPT algorithm**

327 Odor sensing plays an important role in situations in which visual search is difficult (a space filled
328 with darkness and thick smoke). However, because the technology for development of an odor
329 sensor is lagging behind that of other sensory sensors (e.g., cameras, microphones), robot olfac-
330 tory research is still a developing field. Currently, dogs play the role of odor sensors, but due to
331 the high cost of training dogs and the deterioration of their odor sense with physical condition
332 and age, engineering solutions using autonomous mobile robots for searching are needed. Con-
333 ventional robot olfactory research has emphasized the development of motion planning (search
334 algorithm). The search algorithm is roughly divided into two fields: one is a bio-inspired algorithm
335 that imitates the search behavior of living organisms, and the other is a search that estimates the
336 position of the odor source using a statistical method (statistical algorithm). The bio-inspired al-
337 gorithm, which mimics the behavior of organisms that can search in real time, is superior to the
338 statistical algorithm in terms of robot implementation (e.g., (*Russell et al.*, *2003*)(*Lochmatter et al.*,
339 *2008*)). However, behavior patterns and movement speeds in these bio-inspired algorithms are al-
340 ways constant, regardless of the environmental conditions. Accordingly, there was a problem that
341 the original search performance of living things could not be replicated. For this reason, different
342 kinds of research have been carried out more recently and applied to the bio-inspired algorithm,
343 such as information-theoretic analysis of the trajectory of an insect (*Hernandez-Reyes et al.*, *2021*),
344 extraction of adaptability from neuroethology data by fuzzy inference (*Shigaki et al.*, *2019b*), and
345 acquisition of behavioral switching indices in response to environmental changes by measuring in-
346 sect behavior while visualizing airflow (*Demir et al.*, *2020*). In this study, we found that behavioral
347 modulation occurred based on the relationship between the direction of the odor arrival and the
348 wind, and we used our data to reproduce a behavioral trajectory that was not only better than that
349 of the conventional bio-inspired algorithm, but was also more similar to the search behavior of the
350 actual silkmoth. Therefore, it is clear that a probabilistic and time-varying behavior modulation
351 mechanism has a better search performance than a time-invariant search algorithm.

352 **Materials and methods**

353 **Animals**

354 Silkmoths, *Bombyx mori* (Lepidoptera: Bombycidae) were purchased from Ehine Sansyu Co., Japan.
355 Adult male moths were cooled at 16°C one day after eclosion to reduce their activity, and were
356 tested within 2–7 days after eclosion. Before the experiments, the moths were kept at room tem-
357 perature (25–28 °C) for at least 10 min.

358 **Virtual odor field**

359 To generate a virtual odor field closely mimicking reality, smoke was emitted into the actual en-
360 vironment. The diffusion of the smoke was recorded and implemented into the simulator using
361 image processing. The smoke visualization experiment was conducted in an approximately 2.5 ×
362 0.8 m area in a darkroom. First, the smoke was visualized using a smoke generator and a laser
363 sheet. The smoke emitted into the room gleamed when it hit the irradiated laser sheet, and the

364 distribution of smoke was recorded using a high-sensitivity camera. In this experiment, we carried
365 out a visualization experiment in a darkroom because it is important to accurately record the light
366 reflected by the smoke. This method was based on particle image velocimetry (PIV), which mea-
367 sures the velocity of fluid flow in space by visualizing particles and analyzing their movements. PIV
368 accuracy is improved by scattering a large amount of smoke (particles) in space because it focuses
369 on accurately tracking each particle, however, our method did not require following each parti-
370 cle. Instead, our method used a mass of smoke as an odor plume, and we observed how smoke
371 floated and was distributed in space. In the visualization experiment, the flow meter (1.0 L/min)
372 and solenoid valve (1 Hz) were controlled under the same released conditions as in the behavioral
373 experiment. Our method required less smoke than does PIV, and the smoke is thinner and more
374 difficult to visualize. For this reason, it was necessary to increase the sensitivity of the camera,
375 however, noise increased accordingly. Moreover, in PIV, it is not necessary to distinguish between
376 smoke particles and dust because only the movement of particles in space is important, but our
377 method required removing other particles in order to measure the smoke position alone as the
378 plume. Hence, we applied image processing to the smoke image. Luminance values can have a
379 large range because the intensity of smoke varies with airflow and time. In addition, it is difficult
380 to extract only smoke with simple thresholding because the noise caused by dust has the same
381 luminance as does smoke. Therefore, we adopted a method that focuses on connected compo-
382 nents to remove noise while maintaining the shape of the smoke. In grouping based on connected
383 components, two objects are considered connected if adjacent pixels in a binary image take the
384 value of 1. Because smoke exists as a mass, it can be inferred that it has an area above a certain
385 level when divided into connected components. For this reason, we removed the pixels whose
386 connected components were not in adjacent pixels and whose area did not exceed a certain level.
387 These processes were performed with source code using OpenCV.

388 **Configuration of virtual reality system**

389 The behavioral experiment was carried out using a homemade virtual reality system (a photograph
390 of the actual device is shown in Fig. 1A). The traditional tethered measurement system is used for
391 behavior measurement, and a stimulator that presents odor, visual, and wind direction informa-
392 tion is installed around the tethered measurement system (Figure 1-Figure supplement 1A). The
393 details of each stimulator are as follows.

394 **Odor stimulator**

395 We provided sex pheromone stimulation to both antennae of a silkworm using Bombykol ((E,Z)-
396 10,12-hexadecadien-1-ol). A cartridge containing 1000 ng of bombykol was placed in a tube in
397 order to present air containing bombykol to the silkworm. The compressed air from the air com-
398 pressor (NIP30L, Nihon Denko, Aichi, Japan) passed through three gas washing bottles containing
399 degreased cotton, activated carbon, and water, respectively, and was adjusted to 1.0 L/min using a
400 flow meter (KZ-7002-05A, AS ONE CORPORATION, Osaka, Japan). The timing of the stimulation was
401 controlled by switching the flow path of the solenoid valve (VT307, SMC Corporation, Tokyo, Japan).
402 The odor stimulus discharge ports were integrated with the tethered rod, and the discharge ports
403 were located above the antennae. The tethered rod with the discharge ports was fabricated using
404 a 3D printer (Guider2, Flashforge 3D Technology Co., Ltd., Zhejiang, China). As a result of present-
405 ing a one-shot pheromone stimulus to the silkworm using this odor stimulator, the odor stimulus
406 can be presented correctly because the female search behavior was elicited (Figure 1-Figure sup-
407 plement 1B).

408 **Vision stimulator**

409 Because the optical flow presentation method using LED arrays was also used in previous studies
410 with flying insects, we also use the same method in this study. The visual stimulus device was
411 constructed by arranging LEDs (WS2812B, WORLDSEMI CO., LIMITED, GuangDong, China) with a

412 built-in microcomputer in an array around the tethered measurement system. The LED array was
413 comprised of 256 LEDs arranged in 8 (vertical) × 32 (horizontal) panels. The array was presented
414 as an optical flow by controlling the lighting timing of each LED according to the angular velocity of
415 the silkmoth.

416 Because it has been reported that the silkmoth causes optomotor reflexes with respect to optical
417 flow and the neck tilts in the direction of optical flow (*Minegishi et al., 2012*), whether or not this
418 vision stimulator is functioning was evaluated by the angle of the neck with respect to optical flow.
419 The vision stimulator is functioning properly because the silkmoth has the largest neck tilt in the
420 range of angular velocity during the female search behavior (Figure 1-Figure supplement 1C), and
421 this result is similar to the past research data (*Pansopha et al., 2014*).

422 Wind stimulator

423 The wind presented to the silkmoths was generated using the push-pull rectifier (*González et al.,*
424 *2008*). The push-pull rectifier consists of a push side that sends out the wind and a pull side that
425 draws in the sent wind. Fans (PMD1204PQB1, SUNON, Takao, Taiwan) were installed on both the
426 push and pull sides to generate airflow. Space can be used effectively using this device because air
427 can flow without covering the workspace with a partition. The push-pull rectifier was connected to a
428 hollow motor (DGM85R-AZAK, ORIENTAL MOTOR Co., Ltd., Tokyo, Japan) which rotated to generate
429 wind. The performance of the push-pull rectifier was evaluated using particle image velocimetry
430 (PIV) (*Adrian, 2005*). For PIV analysis, we used videos that were shot at 800 fps with a resolution of
431 640 × 480 pixels. As a result, it was confirmed that the wind generated by the push-pull rectifier
432 did not generate vortices (Figure 1-Figure supplement 1D).

433 VR system evaluation experiment

434 We experimentally verified the extent to which a VR system equipped with odor, vision, and wind
435 direction stimulators could reproduce a free-walking experiment in a real environment. In the free-
436 walking experiment in a real environment, the search field was the same size as the VR system, and
437 an odor emission frequency (1 Hz) was used. Two repeated experiments were carried out using
438 15 moths, and their behavior was recorded using a 30 fps video camera (BSW200MBK, BUFFALO,
439 Aichi, Japan). The figure shows the results of the quantitative comparison of search success rate
440 and relative distance (Figure 1-Figure supplement 1E, F). We found that there was no difference
441 between the results of VR and the free walking experiment. In other words, VR was able to repro-
442 duce the experiment of free walking, and the behavior experiment may be performed using the
443 VR device proposed in this study.

444 Migration pathway ratio map

445 The migration pathway ratio map statistically processed the trajectories of all trials and denoted
446 the points where the quadcopter frequently passed through the experimental field. We created
447 the migration pathway ratio map $C_n(x, y)$ based on the rule given by Equation (5). Here, n represents
448 the trial number, and the size of a grid cell is 0.1×0.1 .

$$C_n(x, y) = \begin{cases} 1 & : \text{The silkmoth passed through the coordinates } (x, y). \\ 0 & : \text{The silkmoth did not pass through the coordinates } (x, y). \end{cases} \quad (5)$$

449 We applied the equation to all trial trajectories and summarized them, and then calculated the
450 trial average based on equation (5) to create the migration pathway ratio map $P(x, y)$. The migration
451 pathway ratio map was created using MATLAB (2020a, MathWorks, MA, USA).

$$P(x, y) = \frac{\sum_{n=1}^N C_n(x, y)}{N} \quad (6)$$

452 **Statistical Analysis**

453 For all data analyses, R version 4.0.3 was used (R Core Team). All earth mover's distance calculations
454 were performed using the python 3.7 language.

455 **Odor source search algorithm**

456 The details of the three algorithms for which simulation experiments were performed are de-
457 scribed here.

458 surge-zigzagging

459 A surge-zigzagging algorithm models the female search behavior of an adult male silkmoth, which
460 is a walking insect (Figure 5-Figure supplement 1A). In response to a one-shot sex pheromone stim-
461 ulus, the silkmoth exhibits a movement that advances in the direction of the odor and a straight
462 movement (surge), followed by a rotational movement (zigzag/loop) to search for further odor
463 information from all directions. The flow chart of the surge-zigzagging algorithm is shown in the
464 supplementary figures. The surge state in the algorithm lasts for 0.5 seconds because surge behav-
465 ior lasts for about 0.5 seconds after the odor stimulus is presented. Because the surge behavior
466 is elicited when the odor stimulus is presented, the trajectory becomes linear when the odor is
467 continuously (high frequency) presented.

468 casting

469 A casting algorithm models the odor source localization behavior of a flying moth by mapping
470 it onto a two-dimensional plane (*Li et al., 2001*). A schematic diagram of this algorithm and an
471 implemented flowchart are shown in the supplementary figure (Figure 5-Figure supplement 1B).
472 When the agent in this algorithm detects an odor plume, it moves upwind, and when it loses sight
473 of the plume, it moves in the crosswind direction to rediscover the plume. At this time, when
474 moving upwind, it moves at a certain angle β with respect to the upwind direction and continues
475 moving a certain distance d_{lost} after losing sight of the plume. By repeating these movements in the
476 upwind and crosswind directions, the odor source is localized. The parameters of β and d_{lost} are
477 30° and 2.5 cm, respectively, and these coincide with the highest search success rates in previous
478 research (*Lochmatter et al., 2008*).

479 **Acknowledgments**

480 We thank Dr. Takeshi Sakurai (Tokyo University of Agriculture) for providing the sex pheromone,
481 bombykol.

482 **Additional information**

483 **Funding**

Funder	Grant reference number	Author
JSPS KAKENHI	JP19H04930	Shunsuke Shigaki
JSPS KAKENHI	JP19K14943	Shunsuke Shigaki
JSPS KAKENHI	JP19H02104	Daisuke Kurabayashi

The funders had no role in study design, data collection and interpretation,

or the decision to submit the work for publication.

484 **Author contributions**

485 MY, OH and SS, Planned and designed experiments, Conducted experiments, Analysed and inter-
486 preted data, Conception and design, Acquisition of data, Drafting or revising the article; KH and DK,
487 Analysed and interpreted data, Conception and design, Drafting or revising the article

488 **Ethics**

489 Animal experimentation: Study involved experiments on silkmoths and were conducted according
490 to ethical guidelines

491 **References**

- 492 **Adrian RJ**. Twenty years of particle image velocimetry. *Experiments in fluids*. 2005; 39(2):159–169.
- 493 **Berg HC**. *E. coli in Motion*. Springer Science & Business Media; 2008.
- 494 **Celani A**. Olfactory Navigation: Tempo is the key. *Elife*. 2020; 9:e63385.
- 495 **Chen Xx**, Huang J. Odor source localization algorithms on mobile robots: A review and future outlook. *Robotics*
496 *and Autonomous Systems*. 2019; 112:123–136.
- 497 **Crimaldi J**, Koseff J. High-resolution measurements of the spatial and temporal scalar structure of a turbulent
498 plume. *Experiments in Fluids*. 2001; 31(1):90–102.
- 499 **Demir M**, Kadakia N, Anderson HD, Clark DA, Emonet T. Walking *Drosophila* navigate complex plumes using
500 stochastic decisions biased by the timing of odor encounters. *Elife*. 2020; 9:e57524.
- 501 **Dyhr JP**, Higgins CM. The spatial frequency tuning of optic-flow-dependent behaviors in the bumblebee *Bom-*
502 *bus impatiens*. *Journal of Experimental Biology*. 2010; 213(10):1643–1650.
- 503 **Dyhr JP**, Morgansen KA, Daniel TL, Cowan NJ. Flexible strategies for flight control: an active role for the ab-
504 domen. *Journal of Experimental Biology*. 2013; 216(9):1523–1536.
- 505 **Fujiwara T**, Kazawa T, Sakurai T, Fukushima R, Uchino K, Yamagata T, Namiki S, Haupt SS, Kanzaki R. Odorant
506 concentration differentiator for intermittent olfactory signals. *Journal of Neuroscience*. 2014; 34(50):16581–
507 16593.
- 508 **González E**, Marzal F, Miñana A, Doval M. Influence of exhaust hood geometry on the capture efficiency of
509 lateral exhaust and push–pull ventilation systems in surface treatment tanks. *Environmental progress*. 2008;
510 27(3):405–411.
- 511 **Haber Kern H**, Hedwig B. Behavioural integration of auditory and antennal stimulation during phonotaxis in
512 the field cricket *Gryllus bimaculatus*. *Journal of Experimental Biology*. 2016; 219(22):3575–3586.
- 513 **Hernandez-Reyes CA**, Fukushima S, Shigaki S, Kurabayashi D, Sakurai T, Kanzaki R, Sezutsu H. Identification
514 of exploration and exploitation balance in the silkmoth olfactory search behavior by information-theoretic
515 modeling. *Frontiers in Computational Neuroscience*. 2021; 15.
- 516 **Kanzaki R**. Coordination of wing motion and walking suggests common control of zigzag motor program in a
517 male silkworm moth. *Journal of Comparative Physiology A*. 1998; 182(3):267–276.
- 518 **Kaushik PK**, Renz M, Olsson SB. Characterizing long-range search behavior in Diptera using complex 3D virtual
519 environments. *Proceedings of the National Academy of Sciences*. 2020; 117(22):12201–12207.
- 520 **Kikas T**, Ishida H, Webster DR, Janata J. Chemical plume tracking. 1. Chemical information encoding. *Analytical*
521 *chemistry*. 2001; 73(15):3662–3668.
- 522 **Li W**, Farrell JA, Card RT. Tracking of fluid-advected odor plumes: strategies inspired by insect orientation to
523 pheromone. *Adaptive Behavior*. 2001; 9(3-4):143–170.
- 524 **Lochmatter T**, Raemy X, Matthey L, Indra S, Martinoli A. A comparison of casting and spiraling algorithms for
525 odor source localization in laminar flow. In: *2008 IEEE International Conference on Robotics and Automation*
526 *IEEE*; 2008. p. 1138–1143.
- 527 **Lockery SR**. The computational worm: spatial orientation and its neuronal basis in *C. elegans*. *Current opinion*
528 *in neurobiology*. 2011; 21(5):782–790.

- 529 **Minegishi R**, Takashima A, Kurabayashi D, Kanzaki R. Construction of a brain-machine hybrid system to eval-
530 uate adaptability of an insect. *Robotics and Autonomous Systems*. 2012; 60(5):692–699.
- 531 **Murlis J**, Elkinton JS, Carde RT. Odor plumes and how insects use them. *Annual review of entomology*. 1992;
532 37(1):505–532.
- 533 **Murlis J**, Willis MA, Cardé RT. Spatial and temporal structures of pheromone plumes in fields and forests.
534 *Physiological entomology*. 2000; 25(3):211–222.
- 535 **Naik H**, Bastien R, Navab N, Couzin ID. Animals in Virtual Environments. *IEEE Transactions on Visualization*
536 *and Computer Graphics*. 2020; 26(5):2073–2083. doi: [10.1109/TVCG.2020.2973063](https://doi.org/10.1109/TVCG.2020.2973063).
- 537 **OBARA Y**. *Bombyx mori* mating dance: An essential in locating the female. *Applied Entomology and Zoology*.
538 1979; 14(1):130–132.
- 539 **Pansopha P**, Ando N, Kanzaki R. Dynamic use of optic flow during pheromone tracking by the male silkmoth,
540 *Bombyx mori*. *Journal of Experimental Biology*. 2014; 217(10):1811–1820.
- 541 **Renou M**. Pheromones and general odor perception in insects. *Neurobiology of chemical communication*.
542 2014; 1:23–56.
- 543 **Rubner Y**, Guibas LJ, Tomasi C. The earth mover's distance, multi-dimensional scaling, and color-based image
544 retrieval. In: *Proceedings of the ARPA image understanding workshop*, vol. 661; 1997. p. 668.
- 545 **Russell RA**, Bab-Hadiashar A, Shepherd RL, Wallace GG. A comparison of reactive robot chemotaxis algorithms.
546 *Robotics and Autonomous Systems*. 2003; 45(2):83–97.
- 547 **Ryohei K**, Naoko S, Tatsuaki S. Self-generated zigzag turning of *Bombyx mori* males during pheromone-
548 mediated upwind walking. *Zoological science*. 1992; 9(3):515–527.
- 549 **Schmitz B**, Scharstein H, Wendler G. Phonotaxis in *Gryllus campestris* L.(orthoptera, gryllidae). *Journal of*
550 *comparative physiology*. 1982; 148(4):431–444.
- 551 **Shigaki S**, Fukushima S, Kurabayashi D, Sakurai T, Kanzaki R. A novel method for full locomotion compensation
552 of an untethered walking insect. *Bioinspiration & biomimetics*. 2016; 12(1):016005.
- 553 **Shigaki S**, Haigo S, Reyes CH, Sakurai T, Kanzaki R, Kurabayashi D, Sezutsu H. Analysis of the role of wind infor-
554 mation for efficient chemical plume tracing based on optogenetic silkworm moth behavior. *Bioinspiration*
555 *& biomimetics*. 2019; 14(4):046006.
- 556 **Shigaki S**, Sakurai T, Ando N, Kurabayashi D, Kanzaki R. Time-varying moth-inspired algorithm for chemical
557 plume tracing in turbulent environment. *IEEE Robotics and Automation Letters*. 2017; 3(1):76–83.
- 558 **Shigaki S**, Shiota Y, Kurabayashi D, Kanzaki R. Modeling of the Adaptive Chemical Plume Tracing Algorithm of
559 an Insect Using Fuzzy Inference. *IEEE Transactions on Fuzzy Systems*. 2019; 28(1):72–84.
- 560 **Wehner R**. Desert ant navigation: how miniature brains solve complex tasks. *Journal of Comparative Physiology*
561 *A*. 2003; 189(8):579–588.
- 562 **Wyatt TD**. Pheromones and animal behavior: chemical signals and signatures. Cambridge University Press;
563 2014.
- 564 **Yanagawa SS Ryota**, Shiota, Kurabayashi D. Construction of chemical plume tracing simulator in a non-
565 rectifying environment. In: *IEEE*; 2018. p. 147–150.

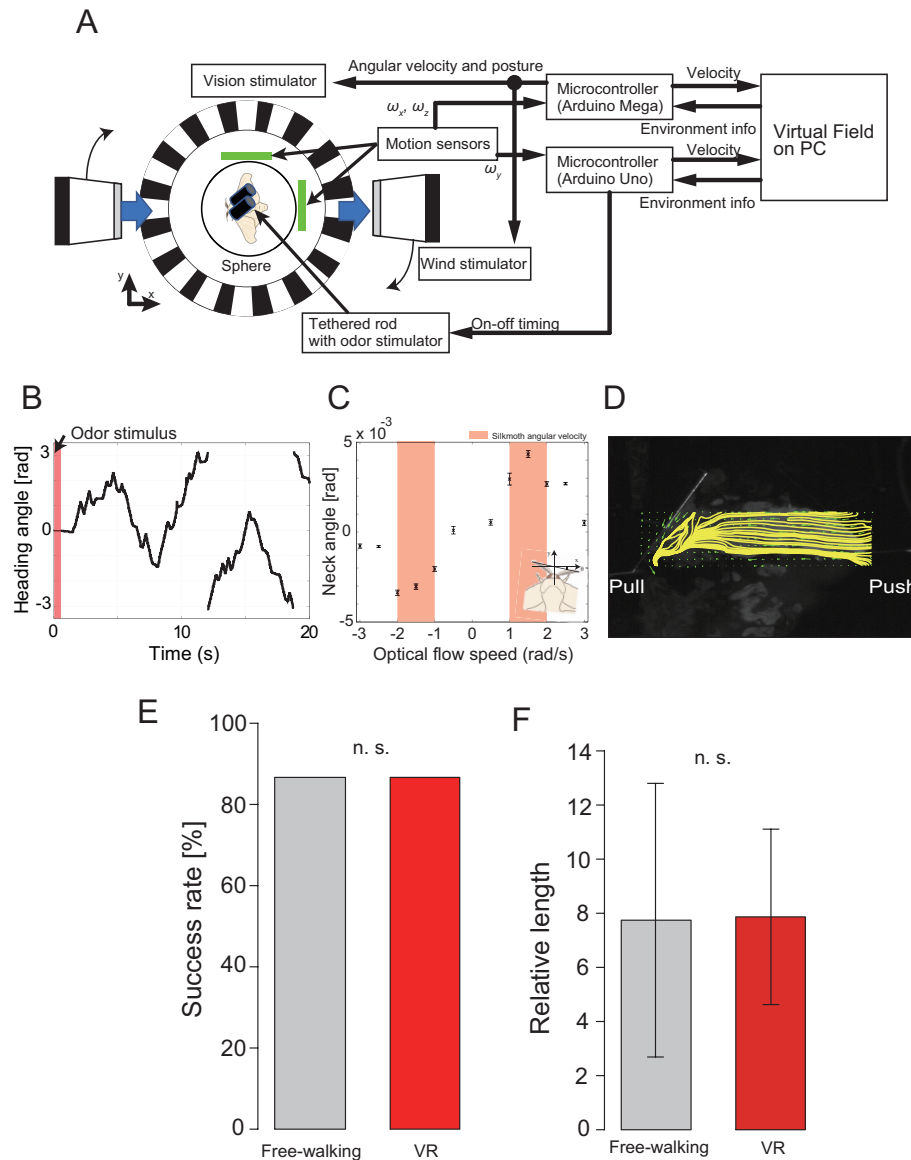


Figure 1-Figure supplement 1. Data comparison between free walking experiment and VR experiment. A: VR system configuration diagram. Two microcomputers were used to control the stimulator and measure the amount of rotation of the sphere. B–D: Evaluation experiment results of each stimulator. B is a graph showing the change in the heading angle of the silkmoth. It was confirmed that when the odor was presented from the upper part of the antennae, the female search behavior was elicited while changing the heading angle significantly. C investigated whether the visual motion reflex was elicited by the visual stimulator by observing the change in the angle of the neck. Because the neck tilt was the largest in the same speed band as the angular velocity of the silk moth, it was confirmed that the visual stimulus could be presented correctly. D is a snapshot of the push-pull rectifier, which is a wind stimulator, visualized by PIV. Since the yellow line represents the streamline and does not generate vortices, it was confirmed that rectification can be generated by push-pull. E: Comparison of search success rates between free walking experiments and VR experiments (Fisher's exact test, $p < 0.05$). The free walking experiment is the result of two repeated experiments using 15 silkmoths ($n = 30$). The environment of the free walking experiment was set to be the same as the virtual environment of the VR system. F: Comparison of a relative length. The relative length is an evaluation value that standardizes the distance actually traveled by the shortest distance to the odor source. This makes it possible to evaluate how much action was taken in response to sensory input. Because there was no difference between free walking and VR (Welch's t-test, $p < 0.05$), it is highly possible that the search behavior expressed by a silkmoth in the VR experiment is the same as the behavior in the free walking experiment.

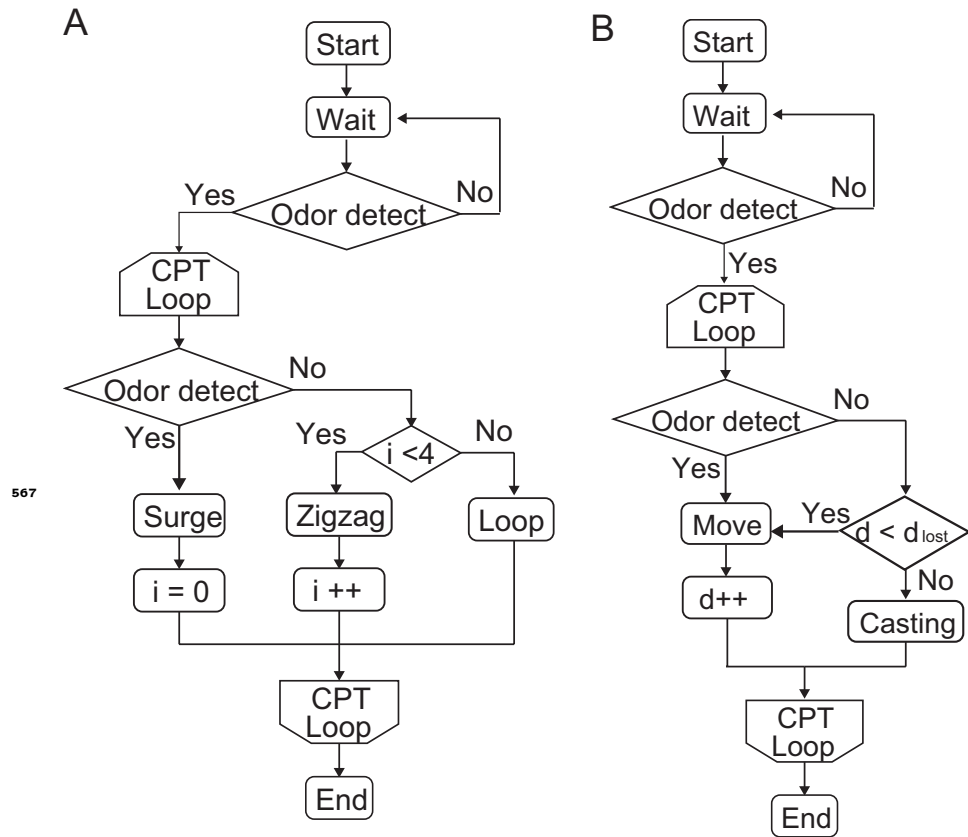


Figure 5-Figure supplement 1. Flowchart of the algorithm used in the simulation experiment. A: Flowchart of the surge-zigzagging algorithm. The surge state and the zigzag/loop state are switched by the odor stimulus. B: Flowchart of the casting algorithm. By detecting the odor, it moves upwind, and when it loses its odor, it casts in the crosswind direction.